



UNIVERSIDAD AUTÓNOMA DE SAN LUIS POTOSÍ
FACULTAD DE CIENCIAS QUÍMICAS
POSGRADO EN CIENCIAS FARMACOBIOLOGICAS



“Design of Bismuth-based Nanostructures with Photocatalytic and Antibacterial Activity”

(Diseño de nanoestructuras basadas en bismuto con actividad fotocatalítica y antibacterial)

TESIS

Para la obtención del título de
Maestra en Ciencias Farmacobiológicas

PRESENTA

Q.F.B GÓMEZ NARVÁEZ BEATRIZ

Dra. Esmeralda Mendoza Mendoza
Co-directora de Tesis

Dr. Fidel Martínez Gutiérrez
Co-director de Tesis

Dr. René Darío Peralta Rodríguez
Asesor

San Luis Potosí, San Luis Potosí, 21 de julio de 2022



El programa de Maestría en Ciencias Farmacobiológicas de la Universidad Autónoma de San Luis Potosí pertenece al Programa Nacional de Posgrados de Calidad (PNPC) del CONACyT, registro 003383, en el Nivel EN DESARROLLO. Número de registro de la beca otorgada por CONACYT: 781924 CVU 1079079

“El financiamiento de este proyecto se realizó a través de los proyectos CONACYT con referencias CB-2016-285350 e INFRA-2018-294130, además del apoyo para acciones de mantenimiento de infraestructura científica, Laboratorio Nacional de Micro y Nanofluídica, LABMYN 2020; proyecto 314907.



Design of Bismuth-based Nanostructures with Photocatalytic and Antibacterial Activity por Beatriz Gómez Narváez, Esmeralda Mendoza Mendoza, René Darío Peralta Rodríguez, Fidel Martínez Gutiérrez se distribuye bajo una [Licencia Creative Commons Atribución-NoComercial-SinDerivadas 4.0 Internacional](https://creativecommons.org/licenses/by-nc-nd/4.0/).



UNIVERSIDAD AUTÓNOMA DE SAN LUIS POTOSÍ
FACULTAD DE CIENCIAS QUÍMICAS
POSGRADO EN CIENCIAS FARMACOBIOLOGICAS



“Design of Bismuth-based Nanostructures with Photocatalytic and Antibacterial Activity.”

(Diseño de nanoestructuras basadas en bismuto con actividad fotocatalítica y antibacterial)

TESIS

Para la obtención del título de

Maestra en Ciencias Farmacobiológicas

PRESENTA

Q.F.B GÓMEZ NARVÁEZ BEATRIZ

SINODALES

Dra. Esmeralda Mendoza Mendoza

Facultad de Ciencias Químicas
Universidad Autónoma de San Luis Potosí

Dr. René Darío Peralta Rodríguez

Centro de Investigación en Química Aplicada
Saltillo, Coahuila.

Dr. Fidel Martínez Gutiérrez

Facultad de Ciencias Químicas
Universidad Autónoma de San Luis Potosí



San Luis Potosí, S.L.P. a 8 de julio, 2022

**Comité Académico del Posgrado
En Ciencias Farmacobiológicas
Facultad de Ciencias Químicas / UASLP
P R E S E N T E.**

Por medio de la presente me permito hacer de su conocimiento que se ha realizado la revisión de la tesis titulada: "Diseño de nanoestructuras basadas en bismuto con actividad fotocatalítica y antibacterial" a favor de la estudiante Q.F.B. Beatriz Gómez Narváez del Posgrado en Ciencias Farmacobiológicas en la modalidad de Maestría para obtener el título de MAESTRA EN CIENCIAS FARMACOBIOLOGICAS.

Por lo que no tenemos ningún inconveniente en emitir la presente CARTA DE APROBACIÓN, a fin de que prosiga con los trámites correspondientes a sustentar su examen profesional.

Sin otro particular nos mantenemos atentos a cualquier requerimiento.

ATENTAMENTE:

**Dr. Fidel Martínez Gutiérrez
Co-director de Tesis**

**Dra. Esmeralda Mendoza Mendoza
Co-directora de Tesis**

**Dr. René Darío Peralta Rodríguez
Asesor**



**FACULTAD DE
CIENCIAS QUÍMICAS**
Dr. Manuel Navo Núm. 6
Zona Universitaria-CP78210
San Luis Potosí, S.L.P.
tel. (444) 826 24 40 al 46
fax (444) 826 2372
www.uaslp.mx

Dedication

To all the people who were always by my side for support and their trust on me, specially to my parents Beatriz Narváez and Martin Gómez, to my siblings Ana Maria and Martin. To Edgar Armendáriz for encouraging me to never surrender and for its patience. To my friends Lucero Ruíz, Cecilia Flores, Selene Velázquez, and Abraham Echeverria for its unvaluable support and words of encouragement.

Acknowledgements

I want to express my greatest gratitude to my thesis directors Dr. Esmeralda Mendoza Mendoza, Dr. René Darío Peralta Rodríguez and Dr. Fidel Martínez Gutiérrez for their unvaluable support, compromise, enthusiasm and patience that led to the successful culmination of this investigation.

I want to acknowledge my colleagues from the Advance Materials Laboratory for its support and fellowship, to Dr. Sonia Segovia Sandoval, I.Q. Cecilia Flores Cardona, L.Q. Katya Gómez Villegas, INER Marisol Pérez González, INER Daniel Camacho Ventura and I.Q. Abraham López Cano.

I want to acknowledge my colleagues from the Antimicrobial Biofilms and Microbiota for its guide, M.C. Miguel Angel Álvarez Zapata, M.C. Montserrat López Carrizales, M.C. Selene Velázquez Moreno, M.C. Sara Almendárez Luna, and M.C. Ana Maria. Thanks to the technical personnel of the Medic Genomic Laboratory, to M.C. Perla Yazmin Rodríguez Martínez and Dr. Pedro Gerardo Hernández Sánchez.

My sincere thanks to the professionalizing project students, Dolores, Fernanda, Carolina, Ana Isabel, Ximena, Linda, and Sarahi. For all the gratifying moments of learning that we spent together.

Thanks to the Consejo Nacional de Ciencia y Tecnología (CONACYT) for the master's degree scholarship No. 781924.

This thesis could not have been completed without the financial support of the CONACYT through the project CB-2016-285350 and INFRA-2018-294130.

Resumen

En el presente trabajo se sintetizaron y decoraron nanoestructuras (NEs) de vanadato de bismuto (BiVO_4 -NEs) con grafeno (G) y plata (Ag): BiVO_4 , G/ BiVO_4 , Ag/ BiVO_4 y G/Ag/ BiVO_4 con el objetivo de fotodegradar colorantes como cristal violeta (CV) e inactivar bacterias representativas (*E. coli*) mediante exposición a luz visible basadas en lámparas LEDs. El porcentaje de degradación de CV logrado por las NEs varió de 73 a 100 % en 180 min. La fotoinactivación de *E. coli* al 100% se logró en 60 min de irradiación con Ag/ BiVO_4 y en 180 min con G/Ag/ BiVO_4 . La NE que exhibió el desempeño más alto en la fotodegradación de CV y la inactivación de *E. coli* fue G/Ag/ BiVO_4 . Se determinaron las especies oxidativas principales causantes de la fotodegradación y fotoinactivación usando las NE sintetizadas y, además, se confirmó su estabilidad química y posible reuso.

Palabras clave.

BiVO_4 ; síntesis; fotocatalisis; cristal violeta; fotoinactivación de *E. coli*.

Abstract

In the present work, bismuth vanadate nanostructures (BiVO_4 -NSs) were synthesized and decorated with graphene (N-G) and silver (Ag): BiVO_4 , G/ BiVO_4 , Ag/ BiVO_4 and G/Ag/ BiVO_4 with the aim to photodegrade dyes such as Crystal Violet (VC) and photoinactivate the bacteria (*E. coli*) as a model, using visible LEDs lamp irradiation. The percent degradation of VC achieved by NSs varied from 73 to 100 % within 180 min. The photoinactivation of *E. coli* (100 %) was achieved in 60 min of irradiation with Ag/ BiVO_4 and in 180 min using G/Ag/ BiVO_4 . The NS that exhibited the highest performance in VC photodegradation and *E. coli* inactivation was G/Ag/ BiVO_4 . The main oxidative species causing the photodegradation and photoinactivation over the NSs was determined and their chemical stability and possibility of reuse was investigated.

Keywords

BiVO_4 ; synthesis; photocatalysis; crystal violet; *E. coli* photoinactivation.

Index

Introduction	1
Background	1
Justification	2
Hypothesis	3
General objective.....	3
Specific objectives.....	3
Materials and methods	4
Synthesis of BiVO ₄ -based photocatalysts.....	4
Photocatalytic antibacterial test	5
Photocatalytic degradation test.....	6
Characterization methods.....	7
Results and discussion.....	9
Characterization of materials	9
Photoinactivation tests	13
Photodegradation tests	15
Conclusions	17
References	18

Introduction

Water pollution is a serious environmental problem which is partially resolved by conventional methodologies and processes that eliminate a major part of pollutants. The methods used, such as membrane processing, flocculation and sedimentation are limited on their application and possess some drawbacks [1] [2] [3]. The most important limitation is the treatment of water with residual inorganic and organic pollutants in already treated textile and pharmaceutical industry effluents, and persistent pollutants in household wastewater due to the consumption of drugs. The discharge of these residual waters causes a serious pollution of water sources [4]. Persistent pollutants represent a major risk for the environment and health care because they can bio-accumulate, and bio-magnify its effects. A growing generation and hence an increasing release to the environment is a consequence of the rapid increase of industrial modernization. These pollutants generated by the pharmaceutical and textile industries remain in trace quantities in wastewater treatment plants and could generate antimicrobial resistance and antibiotic resistant bacteria as well as eco-toxicity. The presence of pathogenic bacteria, drugs and organic compounds in water represents a risk for health care. The main problem in the persistence of antimicrobial agents is the appearance of bacteria resistance. The OMS estimates that for the year 2050 the antimicrobial resistance will cause 10 million deaths around the world.

Background

The development of technologies to control water contamination at low cost and efficiently, is a very important initiative from the sustainable development point of view. Semiconductor-based photocatalysis is an innovative option that satisfies the above-mentioned requirements.

Photocatalysis is a cost-efficient and non-toxic technique that allows the elimination of the persistent pollutants [5]. Some materials commonly used as photocatalyst are TiO_2 , Cu_2O , BiVO_4 , Bi_2WO_6 [6] that, although efficient, its use in photocatalysis is

restricted by the limiting absorption range and the efficient recombination of the exciton generated during the photocatalysis process. Recently, the design of new materials with a broad absorption band in the UV-Vis interval, BiVO_4 and other Bi-based (Bi_2WO_6 , BiO_3 , BOI) have been studied due to their high photocatalytic activity and its wide energy gap (E_g) varying from 1.8 to 3.3 eV.

Justification

Nevertheless, existing photocatalysts require the improvement of the photoinduced charge separation and migration, which are achieved by some methods as the formation of heterostructures and the deposition of noble metal nanoparticles (AgNPs and AuNPs). The deposited particles allow the separation of photoinduced charges while increasing the efficiency of light absorption due to the local surface plasmon resonance (LSPR). Also, to increase the range of absorption of the photocatalyst, some investigations have used materials as multilayered graphene, due to its quantum confinement effect. Nitrogen doping of carbon (N-G) materials has been shown to enhance the electron transfer capability and photocatalytic activity. Besides, N-G materials have been used to achieve full spectrum light absorption even reaching the near infrared. Nitrogen doping is beneficial to improve the optical and electron transfer properties of carbon-based materials.

In this study, a synergistic functional material was proposed to eliminate persistent pollutants in water treatment processes. A combination of materials and its effects on the photocatalytic and antimicrobial performance was studied. The system consists of the surface modification of BiVO_4 synthesized by a hydrothermal method, with the N-graphene and Ag nanoparticles.

Hypothesis

The decoration of bismuth vanadate (BiVO_4) with Ag nanoparticles and N-doped graphene will enhance the degradation of micropollutants (dyes) and the inactivation of pathogenic bacteria in water by means of a synergistic effect.

General objective

Synthesize and characterize bismuth-based nanostructures (N-G/Ag/BiVO_4) to evaluate the degradation of micropollutants and the inactivation of bacteria in aqueous solution by photocatalysis.

Specific objectives

- Synthesize BiVO_4 based nanostructures and modify its surface by the deposition of Ag nanoparticles and N-doped graphene, using green chemistry.
- Characterize the as-synthesized materials by means of different analytical techniques.
- Evaluate the photocatalytic activity to degrade CV using the synthesized materials.
- Study the photoinactivation of *E.coli* (ATCC 25922) bacteria using the synthesized nanostructure materials.

Materials and methods

This section describes the methods used to synthesize the BiVO₄-based photocatalysts and the procedures used to evaluate the antibacterial activity and degradation of dyes via photocatalysis. This section also describes the methods used to characterize and evaluate the physicochemical properties of the as-synthesized materials.

Synthesis of BiVO₄-based photocatalysts

BiVO₄ photocatalysts

BiVO₄ was synthesized in three steps; in the first step, two solutions called solution A and B were prepared, containing the diluted precursors of Bi and V. The second step is the mixing of the solutions A and B, giving solution C, followed by stirring, and pH adjustment to precipitate a yellowish precursor of BiVO₄ which will be treated in the third step in a stainless-steel autoclave reactor at 180°C for 12 h to form the final BiVO₄. Then, the obtained suspension was cooled to room temperature, and the solid was separated by centrifugation and washed with deionized water and ethanol to eliminate unwanted residuals. After that, the product was dried at 60 °C for 24 h.

Photo-deposition of Ag nanoparticles on BiVO₄ photocatalyst surface.

BiVO₄ particles were decorated with Ag nanoparticles using the photo-deposition method. A greenish dispersion was obtained, the solid was recovered by centrifugation and then washed with deionized water and alcohol. This solid was dried at 60 °C for 24 h.

N-doped Graphene (N-G)

The N-doped graphene was synthesized modifying the methodology reported by Mohamed et al. [7]. The material was cooled to room temperature and washed six times with deionized water. The final product was dried in an oven for 63 h.

N-G/BiVO₄

N-G/BiVO₄ was synthesized using a hydrothermal method. The product obtained was rinsed with ethanol and deionized water, then the material was dried at 60 °C for 24 h. The final product acquired a dark yellowish color.

N-G/Ag/BiVO₄

N-G/Ag/BiVO₄ was synthesized in two steps; the first step consisted of the synthesis of N-G/BiVO₄ by the method mentioned above, in the second step the N-G-BiVO₄ was subjected to the photo-deposition of Ag nanoparticles using the same methodology and quantities described above. The resulting material acquired a brown-greenish color.

Photocatalytic antibacterial test

Procedure

Antibacterial activity of the synthesized materials was evaluated using the reference *E. coli* strain ATCC 25922. The materials used in this test was previously sterilized at 121 °C for 20 min in an autoclave. The test was carried out under blue LEDs light irradiation. The bacterial cells were suspended in a solution (HEPES 10 mM and Glucose at 1 %wt) at a concentration of 1.5 x10⁸ colony forming units (CFU) per mL. This suspension was kept under LEDs light while stirred at 500 rpm. A sample of the

suspension was extracted at different time intervals and cells countings were carried out by the Miles-Misra method, in nutrient agar plates, incubated at 37 °C for 24 h.

Re-use cycles

The NSs stability was evaluated with re-use cycles. The results were compared with three different control samples, the first one was processed without light and with photocatalyst, the second one was processed with just light, and the third one without light and without photocatalyst.

Measurement of principal active species

Radicals that play roles in the antibacterial reaction were analyzed by conducting trapping experiments. Then the photoinactivation experiment was carried out in each tube where reactive species quenchers were dropped. And the elimination of the effect of these principal reactive species allowed to propose a mechanism of action. To eliminate the effect of scavengers alone, control experiments with just scavengers and bacteria under UV light were carried out.

Photocatalytic degradation test

General procedure

Photodegradation was carried out using a contaminated solution of CV with a known initial concentration, which was mixed with photocatalyst, under dark conditions to establish the absorption-desorption equilibrium between dye and the photocatalyst surface. Photodegradation was achieved by irradiating the solution with blue LEDs. Then, to quantify the CV remanent concentration at the end of each experiment, aliquots of sample were obtained at different time steps and the temperature was

recorded. The aliquots were centrifugated for removing the photocatalyst and then analyzed by the UV-Vis a spectrometer Shimadzu model UV-1900.

Re-use cycles

The re-use cycle capacity of materials was evaluated by reconditioning the photocatalysts after each use. This process considers washing NSs four times with absolute ethanol used for removing the adsorbed dye.

Measurement of main oxidative species

The principal oxidative species involved in the CV photodegradation were determined by the same photocatalytic experiments but incorporating different radical scavengers. The species used were isopropyl alcohol (IPA) (scavenger of h^+), disodium salt dihydrate (EDTA- Na_2) (scavenger of $\bullet OH$) and ascorbic acid (scavenger of O^{2-}).

Characterization methods

This section describes the different techniques used to characterize the properties of the as-synthesized materials. The structural properties were characterized by X-ray diffraction, transmission electron microscopy and Raman spectroscopy. The physico-chemical properties were evaluated by zeta potential, UV-Vis spectroscopy of diffuse reflectance, photoluminescence and physisorption of N_2 . These characterization methods were carried out to study the relationship between the properties of materials and its effects on the antibacterial and degradation photocatalytic activity. Thus, establishing the properties that possess the main influence in the material performance.

Structural properties by XRD and Raman spectroscopy

The material phases of the synthesized NSs were identified by the XRD technique, using the diffractometer model Rigaku Ultima IV equipped with D/teX detector and monochromatic radiation of Cu K α with a wavelength of $\lambda = 0.154$ nm operated at 40 kV and 44 mA. The cell parameter and crystallite size were obtained by the Halder-Wagner method [8].

Vibrational modes of the BiVO $_4$ and the NSs incorporated with N-G were determined by Raman spectroscopy analysis. Raman spectra were acquired in a Horiba Xplora Plus spectrometer using a 532 nm laser in the wavelength range of 150 –1750 cm $^{-1}$. This technique allows the monitoring of the ID/IG bands of graphene containing NNs, which is related to the degree of disorder and hence affects the properties of the overall composite material. This method was used to characterize the effect of the synthesis conditions and the interaction between the components of composite materials.

Physico-chemical properties by zeta potential, UV-Vis, photoluminescence and N $_2$ physisorption.

The pH at which the net charge of particles surface is equal to zero (pH $_{PIE}$) was evaluated by the zeta potential technique. The equipment used is the Malvern Zetasizer Nano ZS90. The pH $_{PIE}$ was evaluated by the intersection of zero potential and the polynomial adjustment of data at a given pH value.

The UV-Vis absorption light properties of the materials synthesized were evaluated by differential reflectance spectroscopy (DRS) technique with an ISR 2600 Plus integration sphere (220–1400 nm) attached to a Shimadzu 2600 UV–Vis spectrophotometer. This technique allowed the determination of the energy gap (E $_g$) by the Kubelka-Munk method, which is based in the following expression [9].

$$F(R) = \frac{(1 - R)^2}{2R}$$

Were R being the reflectance and $F(R)$ is proportional to the extinction coefficient α . Due to the indirect transition of electronic states in BiVO_4 , the Kubelka-Munk method is modified, and the $F(R)$ function multiplies the photon energy ($h\nu$) in the formula ($F(R) h\nu^n$), using the coefficient of ($n = 1/2$) for the BiVO_4 . The E_g values were determined by extrapolating to zero the linear portion of the ($F(R) h\nu^{1/2}$) curve versus $h\nu$ [9][10][11].

The effects of the energy transfer on the electron-hole pair lifetime were evaluated by the photoluminescence responses, which was evaluated with the equipment Agilent Cary Eclipse. The emission spectra were obtained with an excitation of light of wavelength of $\lambda = 334$ nm, whereas the emission intensity was monitored as function of the different conditions and components on the composite material.

Texture properties as specific area, pore volume and pore diameter were determined through N_2 physisorption characterization. The equipment used was a Micrometrics analyzer model ASAP 2020. The specific surface area was determined by the Brunauer-Emmet-Teller (BET) method. The results allowed to assessed the pore diameter and volume using the Barret-Joyner-Halenda (BJH) method.

Results and discussion

This section contains the results of the characterization of materials, along with its interpretation and discussion. With the aim to correlate the NSs configuration and properties with the photocatalytic antibacterial activity and photocatalytic degradation test results.

Characterization of materials

X-Rays diffraction

Fig. 1 shows the XRD patterns of the synthesized photocatalysts. All samples show the monoclinic scheelite BiVO_4 (BV) phase (JCPDS 75-2480), the Miller indices of the principal planes are in brackets. In samples containing silver nanoparticles Ag/BV and N-G/Ag/BV, it can be seen the principal reflection of cubic Ag, this reflection centered at 38° possesses a low intensity due to the low concentration in the photocatalysts (8 wt%). No other peaks of reflections of impurities were observed.

Fig. 1 XRD patterns of the synthesized samples.

Raman spectroscopy analysis

Fig. 2 shows the Raman spectra of the synthesized BiVO₄-based photocatalysts in the range of 150-1000 cm⁻¹. All NSs (BV, Ag/BV, N-G/BV and N-G/Ag/BV) present the vibrational modes located around 182 cm⁻¹ (A_g^3), 332 cm⁻¹ (A_g^4), 364 cm⁻¹ (A_g^5) and 805 cm⁻¹ (A_g^8) which are associated with monoclinic-scheelite BiVO₄ characteristic vibrational modes [9][12]. The spectrum of N-G, N-G/BV and N-G/Ag/BV presents the characteristic D and G bands at $\approx 1,350$ and $\approx 1,580$ cm⁻¹. The D band is originated by the degree of disorder and local defects in sp² hybridized carbon systems and the G band is originated by in-plane C-C atom stretching vibrations present in graphitic materials. The G-band is highly sensitive to strain effects in sp² nano carbons, it is sensitive to the strain caused by interaction with a substrate, between graphene layers and other external perturbations. The ID/IG intensity ratio is used to quantify disorder in a G monolayer [13]. The ID/IG ratio of intensities in the as synthesized N-G was 1.27, and it decreased for the sample N-G/BV (0.72) and reached its lowest value of 0.58 for the sample N-G/Ag/BV.

Fig. 2 Raman spectra of the as synthesized photocatalysts.

Zeta potential

Fig. 3 shows the dependence of zeta potential on the pH of the suspension. The isoelectric points in all the photocatalysts lie in the range of 2.75 to 4.13 pH units. The values are 3.66 for BV, 4.13 for Ag/BV, 2.75 for N-G/BV and 3.12 for N-G/Ag/BV.

Fig. 3 pH influence in zeta potential of the photocatalysts. pH of isoelectric point (pH_{IEP}) in mV.

UV-Vis DR spectroscopy

Fig. 4 (a) shows the UV-Vis diffuse absorbance spectrum of the synthesized photocatalysts. The BiVO_4 as synthesized shows a strong absorption band in the UV region; the incorporation of Ag nanoparticles onto the surface of these materials increases the photo response in the visible light region, this is due to the effect of the surface plasmon resonance (SPR) of Ag nanoparticles. The E_g values were obtained using the Kubelka-Munk method as stated in the work of Moral-Rodriguez et al. [9]

Fig. 4 UV-Vis Diffuse absorbance spectra (a) and E_g determination of the photocatalysts (b).

Photoluminescence

Photoluminescence measurements shown in Fig. 5 were used to determine the separation efficiency of photogenerated electron hole pairs. The higher intensity of PL the lowest efficiency of separation of photo-generated electron-hole pairs, as a consequence, the weaker photocatalytic activity [14]. All samples were excited with a wavelength of 340 nm at room temperature and its emission intensity was measured in the range of 400 - 580 nm.

Fig. 5 Photoluminescence spectra of the as-prepared photocatalysts at room temperature.

Physisorption of N₂

Texture properties

Table 1 shows the surface area (S_{BET}) values of as-synthesized BiVO₄-NSs which are in the range of 2.5 to 3.56 m²/g, and are of the same order of magnitude as the results reported by Dong et al. [15]. Although a higher S_{BET} specific surface area is beneficial for the photocatalytic performance, the slight loss of specific surface area for the materials decorated with N-G and Ag does not decrease the overall activity, due to the incorporation of N-G and Ag materials as active centers for the photocatalytic and photoinactivation activity by themselves [16].

Table 1 Texture properties obtained by N₂ physisorption.

Fig. 6 shows the N₂ adsorption-desorption isotherms of NSs. According to the International Union of Basic and Applied Chemistry (IUPAC), they all behave similar to type II isotherm which is characteristic of non-porous or macroporous materials. All NSs isotherms exhibit a narrow hysteresis cycle of type H₃ according to the IUPAC classification [17]. The mean pore diameters (D_p) of BiVO₄-NSs are reported in Table 1.

Fig. 6 Adsorption-desorption isotherms of N₂ on BiVO₄-NEs

Photoinactivation tests

Fig. 7 shows the comparison of the antibacterial efficiency of the photocatalysts synthesized used to inactivate *E. coli*, taken as a representative Gram negative bacteria involved in water contamination. Blue LEDs light and obscurity controls showed that *E.*

coli is not deactivated when there is no photocatalyst in the system. All photocatalysts except BiVO₄ present 100 % of antibacterial activity at 180 min of irradiation. Ag surface decorating and N-G enhance the activity of the BiVO₄, the release of activity is accomplished by the synergy between photocatalytic activity of photocatalyst and the antibacterial activity of the Ag nanoparticles, nevertheless the major contribution is the photocatalytic activity [18].

Fig. 7 Inactivation of E. coli by different photocatalysts.

Re-use cycles

Experimental results shown in Fig. 8 show the photocatalytic antibacterial stability of N-G/Ag/BV after three re-use cycles. After the first cycle the sample reduces the antibacterial capacity in 2 Log₁₀, and for a second cycle the N-G/Ag/BV sample does not show antibacterial activity.

Fig. 8 Photocatalytic stability of N-G/Ag/BV against photo deactivation of E. coli.

Reactive oxidative species analysis

Active species analysis plays an important role and is studied to allow defining the possible photocatalytic action mechanism. The results are shown in Fig. 9. The antibacterial activity decreases with EDTA and ascorbic acid. It suggests that the main reactive species are O²⁻ and •OH.

Fig. 9 Photoinactivation of E. coli with N-G/Ag/BV in contact with the different reactants Ascorbic acid (O²⁻), isopropanol (IPA, h⁺), ethylenediaminetetraacetic acid (EDTA, •OH).

Photodegradation tests

Fig. 10a shows the dimensionless VC concentration decay curves (C/C_0) versus irradiation time for the CV degradation in presence of the as-synthesized BiVO_4 -based NSs. An experiment without photocatalyst named as no photolysis was carried out and it showed that the VC molecule is susceptible to being degraded in 3 %, thus the VC molecule is stable under irradiation conditions. The BiVO_4 -NSs that exhibited the greatest photodegradation activity were Ag/BV and N-G/Ag/BV, reaching a degradation of 95 % and 100 %, respectively. This coupling facilitates the charge separation and hinders the recombination of photogenerated pairs. Table 2 contains the percent degradation $\text{VC}(\%X_{\text{VC}})$, the kinetic rate constant k_1 and the correlation coefficient (R^2) of the different photocatalysts. Fig. 10b shows the UV–Vis absorption spectra of VC solution at several irradiation times using the N-G/Ag/BV photocatalyst, it can be seen that after 60 min of irradiation the absorption bands due to VC drop as shown in the inset that contains pictures of the solution after the irradiation time.

Fig. 10 Dimensionless concentration decay curve (C/C_0) versus time ($t = 0-180$ min) for VC degradation in the presence of the as-prepared BiVO_4 photocatalysts (a); UV–Vis absorption spectra of VC solution at several irradiation times using the N-G/Ag/BV photocatalyst (b)

Table 2 kinetic parameters of VC degradation test

Fig. 11a and b show the trapping experiments used to determine the main oxidative species causing CV degradation through the two materials that showed the best photocatalytic activity, Ag/BV and NG/Ag/BV. It is shown in both figures that when ascorbic acid (O^{2-} scavenger agent) is added to the CV solution, the degradation is 29% and 43%. When EDTA- Na_2 is added (h^+ scavenger) the percentage of degradation



presents increases of 81% and 55%, and when IPA is added ($\bullet\text{OH}$ scavenger) the percentage of degradation lies between 94 and 95%, all these percentages respectively to the mentioned photocatalysts. Here, super oxides (O^{2-}) and holes (h^+) are the main species responsible for the photocatalytic degradation of VC and where $\bullet\text{OH}$ radicals do not affect the photodegradation process. These results agree with the results of photoinactivation of *E. coli*.

Fig. 11 Trapping experiments used to determine the main oxidative species causing VC degradation.

For N-G/Ag/BV NS, the photo-generated electrons could migrate to N-G/Ag and generate a reduction of O^2 to yield superoxide radical (O^{2-}) and hydroxyl radical ($\bullet\text{OH}$), which subsequently degrade the VC dye molecules [19]. Therefore, the N-G/Ag/ BiVO_4 NS can enhance the photocatalytic activity of BiVO_4 through the enhanced lifetime of photogenerated electrons/holes above to the specific surface area effect [14].

Re-use cycles

Fig. 12 showed the photodegradation performances of VC in four cycling tests. Here, the degradation efficiency of N-G/Ag/BV was about 92 % after four cycles, indicating an excellent stability and reusability of the as-synthesized photocatalyst. These low decrease in photocatalytic efficiency could be attributed to the increase of occupied adsorption sites after the reconditioning process or a possible small mass loss of Ag and N-G materials on the BiVO_4 surface during the recovering after each cycle [20][21] [22].

Fig. 12 The reusability of Ag/BV  and N-G/Ag/BV  for photocatalytic degradation of VC after four cycling tests.

Conclusions

In this work BiVO₄ based photocatalyst were successfully synthesized via a hydrothermal green synthesis method and decorated with Ag nanoparticles and nitrogen doped graphene. The ternary material N-G/Ag/BiVO₄ showed enhanced photocatalytic and photoinactivation activity under blue LEDs light irradiation.

The VC photodegradation rate order was as follows: N-G/BV < BV < Ag/BV < N-G/Ag/BV.

The *E. coli* degradation rate order was as follows: BV < N-G/BV < N-G/Ag/BV < Ag/BV.

N-G/Ag/BiVO₄ achieved 100 % of photoinactivation activity of *E. Coli* in 3 h, and the 100 % of photodegradation of VC in 60 min.

The k_1 value of N-G/Ag/BV is 4, 2.4 and 7.3 times higher than the k_1 values of BV, Ag/BV and N-G/BV, respectively.

The SPR phenomenon of Ag enhance the visible absorption, increasing the photocatalytic activity and facilitating the separation of photoinduced charge carriers in the photocatalyst. Besides, N-G increases the mobility of electrons and holes and hinders their recombination.

Scavenger tests showed that O²⁻ and h⁺ play the most important roles in the photocatalytic oxidation reaction.

The high stability of the photocatalysts Ag/BV and N-G/Ag/BiVO₄ showed in re-use cycles make it a potential candidate in the field of wastewater treatment.

References

- [1] A. Yusuf *et al.*, “A review of emerging trends in membrane science and technology for sustainable water treatment,” *J. Clean. Prod.*, vol. 266, p. 121867, Sep. 2020, doi: 10.1016/J.JCLEPRO.2020.121867.
- [2] H. Sultana, M. Usman, and Z. H. Farooqi, “Micellar flocculation for the treatment of synthetic dyestuff effluent: Kinetic, thermodynamic and mechanistic insights,” *J. Mol. Liq.*, vol. 344, p. 117964, Dec. 2021, doi: 10.1016/J.MOLLIQ.2021.117964.
- [3] H. Demissie *et al.*, “Advances in micro interfacial phenomena of adsorptive micellar flocculation: Principles and application for water treatment,” *Water Res.*, vol. 202, p. 117414, Sep. 2021, doi: 10.1016/J.WATRES.2021.117414.
- [4] C. Orona-Návar *et al.*, “Removal of pharmaceutically active compounds (PhACs) and bacteria inactivation from urban wastewater effluents by UVA-LED photocatalysis with Gd³⁺ doped BiVO₄,” *J. Environ. Chem. Eng.*, vol. 8, no. 6, p. 104540, Dec. 2020, doi: 10.1016/J.JECE.2020.104540.
- [5] J. Ambigadevi, P. Senthil Kumar, D. V. N. Vo, S. Hari Haran, and T. N. Srinivasa Raghavan, “Recent developments in photocatalytic remediation of textile effluent using semiconductor based nanostructured catalyst: A review,” *J. Environ. Chem. Eng.*, vol. 9, no. 1, p. 104881, Feb. 2021, doi: 10.1016/J.JECE.2020.104881.
- [6] T. Sharifi *et al.*, “Tailored BiVO₄ for enhanced visible-light photocatalytic performance,” *J. Environ. Chem. Eng.*, vol. 9, no. 5, p. 106025, Oct. 2021, doi: 10.1016/J.JECE.2021.106025.
- [7] M. A. A. Mohamed, N. A. Elessawy, F. Carrasco-Marín, and H. A. F. Hamad, “A novel one-pot facile economic approach for the mass synthesis of exfoliated multilayered nitrogen-doped graphene-like nanosheets: new insights into the mechanistic study,” *Phys. Chem. Chem. Phys.*, vol. 21, no. 25, pp. 13611–13622, Jun. 2019, doi: 10.1039/C9CP01418G.
- [8] M. Basak, M. L. Rahman, M. F. Ahmed, B. Biswas, and N. Sharmin, “The use of X-ray diffraction peak profile analysis to determine the structural parameters of cobalt ferrite nanoparticles using Debye-Scherrer, Williamson-Hall, Halder-Wagner and Size-strain plot: Different precipitating agent approach,” *J. Alloys Compd.*, vol. 895, p. 162694, Feb. 2022, doi: 10.1016/J.JALLCOM.2021.162694.
- [9] A. I. Moral-Rodríguez *et al.*, “Novel and green synthesis of BiVO₄ and GO/BiVO₄ photocatalysts for efficient dyes degradation under blue LED illumination,” *Ceram. Int.*, vol. 48, no. 1, pp. 1264–1276, 2022, doi: 10.1016/j.ceramint.2021.09.211.
- [10] M. V. Malashchonak, E. A. Streltsov, D. A. Kuliomin, A. I. Kulak, and A. V. Mazanik, “Monoclinic bismuth vanadate band gap determination by photoelectrochemical spectroscopy,” *Mater. Chem. Phys.*, vol. 201, pp. 189–193, Nov. 2017, doi: 10.1016/J.MATCHEMPHYS.2017.08.053.

- [11] S. Landi, I. R. Segundo, E. Freitas, M. Vasilevskiy, J. Carneiro, and C. J. Tavares, “Use and misuse of the Kubelka-Munk function to obtain the band gap energy from diffuse reflectance measurements,” *Solid State Commun.*, vol. 341, p. 114573, Jan. 2022, doi: 10.1016/J.SSC.2021.114573.
- [12] A. Zhang and J. Zhang, “Hydrothermal processing for obtaining of BiVO₄ nanoparticles,” *Mater. Lett.*, vol. 63, no. 22, pp. 1939–1942, Sep. 2009, doi: 10.1016/J.MATLET.2009.06.013.
- [13] M. S. Dresselhaus, A. Jorio, M. Hofmann, G. Dresselhaus, and R. Saito, “Perspectives on carbon nanotubes and graphene Raman spectroscopy,” *Nano Lett.*, vol. 10, no. 3, pp. 751–758, 2010, doi: 10.1021/nl904286r.
- [14] M. Li, G. Xu, Z. Guan, Y. Wang, H. Yu, and Y. Yu, “Synthesis of Ag/BiVO₄/rGO composite with enhanced photocatalytic degradation of triclosan,” *Sci. Total Environ.*, vol. 664, pp. 230–239, May 2019, doi: 10.1016/J.SCITOTENV.2019.02.027.
- [15] P. Dong, X. Xi, X. Zhang, G. Hou, and R. Guan, “Template-Free Synthesis of Monoclinic BiVO₄ with Porous Structure and Its High Photocatalytic Activity,” *Materials (Basel)*, vol. 9, no. 8, Aug. 2016, doi: 10.3390/MA9080685.
- [16] G. J. Lee, X. Y. Lee, C. Lyu, N. Liu, S. Andandan, and J. J. Wu, “Sonochemical Synthesis of Copper-doped BiVO₄/g-C₃N₄ Nanocomposite Materials for Photocatalytic Degradation of Bisphenol A under Simulated Sunlight Irradiation,” *Nanomaterials*, vol. 10, no. 3, Mar. 2020, doi: 10.3390/NANO10030498.
- [17] M. Thommes *et al.*, “Physisorption of gases, with special reference to the evaluation of surface area and pore size distribution (IUPAC Technical Report),” *Pure Appl. Chem.*, vol. 87, no. 9–10, pp. 1051–1069, Oct. 2015, doi: 10.1515/PAC-2014-1117/PDF.
- [18] M. A. Ahmad, S. Aslam, F. Mustafa, and U. Arshad, “Synergistic antibacterial activity of surfactant free Ag–GO nanocomposites,” *Sci. Rep.*, vol. 11, no. 1, pp. 1–9, 2021, doi: 10.1038/s41598-020-80013-w.
- [19] S. Phanichphant, A. Nakaruk, K. Chansaenpak, and D. Channei, “Evaluating the photocatalytic efficiency of the BiVO₄/rGO photocatalyst,” *Sci. Rep.*, vol. 9, no. 1, Dec. 2019, doi: 10.1038/S41598-019-52589-5.
- [20] Y. Xue, Z. Wu, X. He, Q. Li, X. Yang, and L. Li, “Hierarchical fabrication Z-scheme photocatalyst of BiVO₄ (0 4 0)-Ag@CdS for enhanced photocatalytic properties under simulated sunlight irradiation,” *J. Colloid Interface Sci.*, vol. 548, pp. 293–302, Jul. 2019, doi: 10.1016/J.JCIS.2019.04.043.
- [21] Y. Si *et al.*, “Hierarchical self-assembly of graphene-bridged on AgIO₃/BiVO₄: An efficient heterogeneous photocatalyst with enhanced photodegradation of organic pollutant under visible light,” *J. Alloys Compd.*, vol. 831, p. 154820, Aug. 2020, doi: 10.1016/J.JALLCOM.2020.154820.
- [22] C. Regmi, D. Dhakal, and S. W. Lee, “Visible-light-induced Ag/BiVO₄ semiconductor

with enhanced photocatalytic and antibacterial performance,” *Nanotechnology*, vol. 29, no. 6, 2018, doi: 10.1088/1361-6528/aaa052.